J. Jpn. Soc. Microgravity Appl. Vol. 28 No. 2 2011 (S126–S131)

8th Japan-China-Korea Workshop on Microgravity Sciences for
Asian Microgravity Pre-Symposium

3-D Flow Measurement of Oscillatory Thermocapillary Convection in Liquid Bridge in MEIS

Taishi YANO [1], Koichi NISHINO [1], Hiroshi KAWAMURA [2], Ichiro UENO [3],
Satoshi MATSUMOTO [4], Mitsuru OHNISHI [4] and Shin-ichi YODA [4]

Abstract

Marangoni Experiment in Space (MEIS) has been conducted in the International Space Station (ISS) in order to clarify the transition processes of thermocapillary convection in liquid bridges. The use of microgravity allows us to generate long liquid bridges, 30mm in diameter and up to 60mm in length. Several flow visualization techniques have been applied to those large liquid bridges. 3-D PTV is used to reveal highly three-dimensional flow patterns that appear after the transition. Three CCD cameras are used to observe the motions of the tracer particles from different view angles through the transparent heated disk made of sapphire. Particle images are recorded in the HDD recording system in ISS and they are downloaded to the ground for data analysis. A conventional 3-D PTV technique and a newly-developed multi-frame particle tracking method are combined to obtain the results that can help better understanding of oscillatory 3-D flow fields in the liquid bridges. It is shown that the flow pattern changes from a 2-D axisymmetric steady flow to an oscillatory 3-D non-axisymmetric flow under the supercritical conditions.

1. Introduction

Surface tension difference due to temperature gradient drives the thermocapillary convection (or Marangoni convection). In general, surface tension, σ, negatively depends on the temperature, T, of the working fluid. The driving force, which is caused by the surface tension difference in a non-uniform temperature field, leads to the onset of thermocapillary convection in the direction toward the lower temperature region from higher temperature region (**Fig. 1**). Thermocapillary convection plays an important role in the case where the surface force becomes dominant over the body force (e.g., microgravity environment and small-scale phenomena).

A series of microgravity experiments called Marangoni Experiment in Space (MEIS) started from August 2008 in the Japanese Experiment Module "KIBO" in the International Space Station (ISS)[1)]. The purpose of MEIS is to reveal transition processes of thermocapillary convection in liquid bridges by using several modern measurement techniques. The geometry of the liquid bridge is illustrated in **Fig. 1**. It is known that the thermocapillary convection in a liquid bridge changes from a steady, axisymmetric state to an oscillatory, non-axisymmetric one at the critical condition. This instability is related to many factors, and a large number of studies have been conducted so far.

Two series of space experiments, MEIS-1 and MEIS-2 have been conducted in 2008 and 2009, respectively. In MEIS-1, the critical conditions for the onset of oscillation and oscillation modes have been measured for short liquid bridges. It is found that once the onset of oscillation takes place, the flow pattern changes from two-dimensional (2-D) flow field to three-dimensional (3-D) flow field. However, the associated 3-D flow structures have not been well understood. To reveal 3-D flow structure of thermocapillary convection, 3-D PTV system was used in MEIS-2. 3-D PTV is an effective technique to measure complex 3-D flow fields. This paper reports the method and some results of 3-D flow field measurement of thermocapillary convection in liquid bridges in MEIS-2.

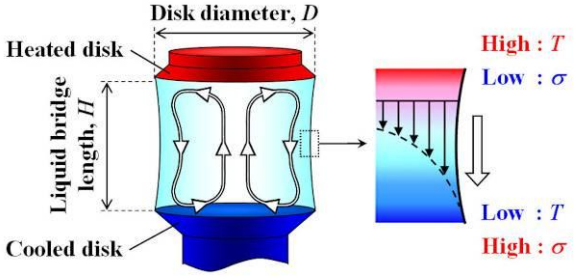

Fig. 1 Illustration of the thermocapillary convection due to temperature gradient

1 Department of Mechanical Engineering, Yokohama National University, 79-5 Tokiwadai, Hodogaya-ku, Yokohama, Kanagawa 240-8501, Japan
2 Faculty of Engineering and Management, Tokyo University of Science, Suwa, 5000-1 Toyohira, Chino, Nagano 391-8502, Japan
3 Faculty of Science and Technology, Tokyo University of Science, 2641 Yamazaki, Noda, Chiba 278-8510, Japan
4 Japan Aerospace Exploration Agency, 2-1-1 Sengen, Tsukuba, Ibaraki 305-8505, Japan
(E mail: nish@ynu.ac.jp)

2. Method

2.1 Fluid Physics Experiment Facility (FPEF)

All the experiments in MEIS were performed in the Fluid Physics Experiment Facility (FPEF). It is operated by the commands sent from the ground. **Figure 2** shows the photos of the receptacle part (right photo) and the exchangeable cassette part (left photo) of FPEF. Measurement apparatuses installed in FPEF are schematically shown in **Fig. 3**. They are a 3-D PTV system, a side-view system, an IR camera, a photochromic dye activation system and fine thermocouples.

Three B/W CCD cameras are placed near the heated disk so that they can observe simultaneously the flow field in the liquid bridge from different angles. The shapes of the liquid bridge and overall flow patterns are viewed by the side-view system with a color CCD camera. Another color CCD camera is installed for the photochromic dye activation technique for surface velocity measurement. Temperature measurements are made with a fine thermocouple sensor and the IR camera.

2.2 Liquid Bridges

In the ground experiments, a syringe needle is used to generate the liquid bridges. But a different method is adopted in MEIS as shown in **Fig. 4**. Two injection holes are drilled in the center of the cooled disk and the working fluid is automatically supplied from the holes as the lower disk is traversed downward.

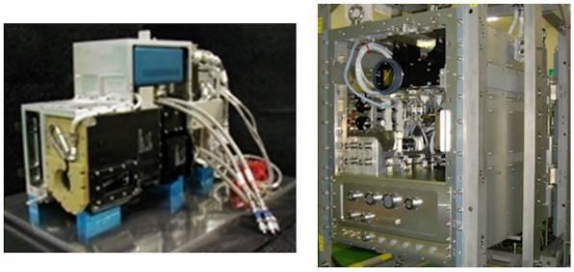

Fig. 2 Receptacle part (right) and exchangeable cassette part (left) of FPEF

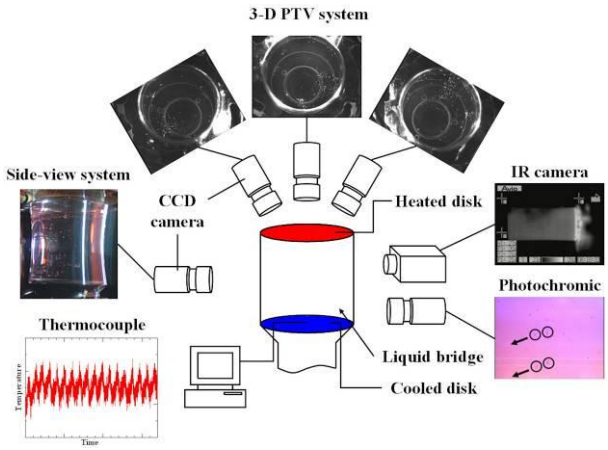

Fig. 3 Schematic diagram of the measurement apparatuses installed in FPEF

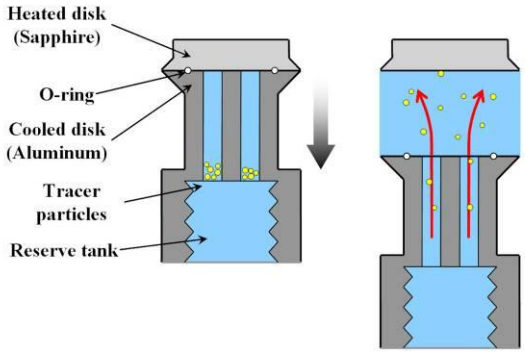

Fig. 4 Injection of tracer particles

The traversing speed is adjusted, so that the stable formation of the liquid bridge is achieved. Tracer particles are introduced into the fluid during the formation of the liquid bridge.

2.3 Experimental conditions

A liquid bridge considered in present study is illustrated in **Fig. 1**. Thermocapillary convection takes place inside the liquid bridge which is suspended between concentric heated and cooled disks. The temperature difference drives the flow that is directed from the heated region to the cooled region at the free surface and then return in the opposite direction in the interior region near the axis of the liquid bridge. The heated disk is made of transparent sapphire with 45-degree edge so that the CCD cameras can observe the flow field through the disk. The cooled disk is made of aluminum. As mentioned above, this lower disk is traversable in the axial direction and a wide range of aspect ratio, Ar (= H / D), can be realized, where H and D are the length of the liquid bridge and the diameter of the disk, respectively. The volume ratio, Vr (= V /V_0), is 0.95, where V and V_0 are the volume of the liquid and that of a cylindrical column ($V_0 = \pi D^2 H/4$). The product of Reynolds number, Re, and Prandtl number, Pr, defines the Marangoni number as follows:

$$Ma = Re \cdot Pr = \frac{|\sigma_T| \Delta T H}{\rho \bar{\nu} \alpha} \tag{1}$$

where σ_T is the temperature coefficient of surface tension, ΔT is the temperature difference between heated and cooled disks, ρ is the density, $\bar{\nu}$ is the mean kinematic viscosity and α is the thermal diffusivity. This Marangoni number is an important parameter for the study of the onset of the oscillation and the subsequent development of 3-D unsteady flow. The onset of oscillation takes place at a critical temperature difference, ΔT_c, which gives a critical Marangoni number, Ma_c, according to Eq. (1).

Silicone oil of 5cSt (=5mm^2/s) in kinematic viscosity and 0.915g/cm^3 in density at 25°C (Shin-Etsu Chemical Co., Ltd,

KF-96L) is used as a working fluid. Its Prandtl number is 67 at 25°C. This fluid is transparent and colorless, thus it is suitable for flow visualization. Approximately 500 tracer particles, whose average diameter and density are respectively 180-200μm and 1.3g/cm^3 are introduced in the fluid. Relatively large particles are selected to facilitate visualization of particle motions for 3-D PTV. Each particle is coated with gold-nickel alloy and the density ratio of the particle to silicone oil is about 1.4. As illustrated in **Fig. 4**, the tracer particles are introduced in the liquid bridge from the injection holes when the liquid bridge is formed.

3. Implementation of 3-D PTV into MEIS

3.1 3-D PTV

3-D PTV is an effective technique to measure 3-D complex flow field, even in the situation of MEIS where many restrictions are imposed on the available resources for the measurement. 3-D PTV measurement of thermocapillary convection in liquid bridges was carried out previously in the ground experiment[2]. Some μg experiments[3)4)] in sounding rockets were also conducted. 3-D PTV measurement requires more than two cameras that observe the motion of tracer particles in the liquid bridge. **Figure 5** shows photos of three CCD cameras mounted in the FPEF, and three particle images taken by the cameras. Geometrical and optical conditions of each camera are determined through the camera calibration, and 3-D particle trajectories are reconstructed from time-consecutive 2-D images acquired. The present 3-D PTV consists of four procedures as follows:

(1) preprocessing of particle images
(2) camera calibration
(3) particle tracking
(4) 3-D reconstruction

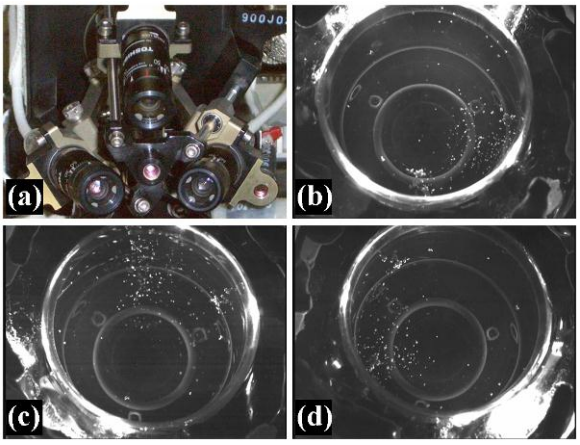

Fig. 5 Photos of (a) Three CCD cameras, and (b)-(d) particle images taken in MIES-2

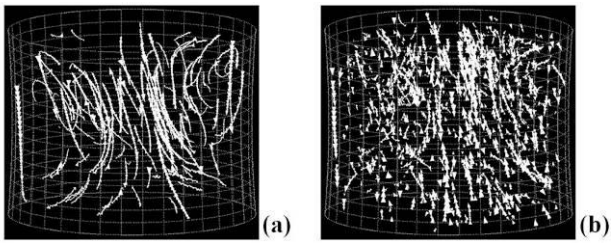

Fig. 6 Results of 3-D PTV using (a) new method, and (b) previous method

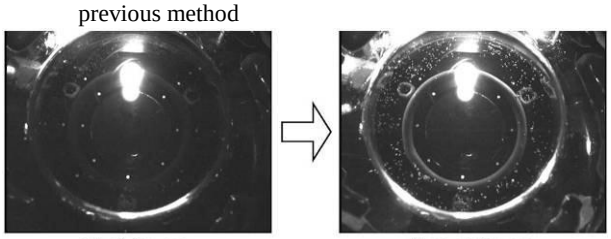

Fig. 7 Blinking of strobe light for time registration

In this study, a new algorithm based on multi-frame particle tracking has been developed[5]. The method for particle tracking is combined with a modified algorithm for 3-D reconstruction for better resolution of flow structures. **Figure 6** compares (a) the present result with (b) the result that would be obtained from the previous algorithm. It is obvious that new method can reduce the number of error vectors and reveal the flow patterns.

3.2 Synchronization of CCD cameras

Particle images taken by three cameras were transferred to the ground and stored as movie files. These movie files must be synchronized to each other because the 3-D PTV needs to extract a set of three particle images taken at the same time as shown in **Figs. 5 (b)-(d)**. To facilitate this synchronization, a blinking period in strobe flashing was given in the beginning of each recording of particle images. **Figure 7** shows the images taken in the blinking period. The left image shows a dark frame taken in a strobe-off period while the right image shows a bright frame taken in a strobe-on period. These dark and bright images can be used as a time reference for synchronization of the movies.

3.3 Camera calibration

For 3-D PTV, it is necessary to determine a set of camera parameters for each camera. The parameters consist of the exterior and interior orientation parameters, where the formers express the translation and rotation of the camera coordinate while the latters express the radial image distortion, the offset of the principle point and the aspect ratio of pixel dimension. In this study, the camera parameters are calculated by the least square method using the equations of the central projection camera model. This model is based on the collinearity condition and it is established previously[6)7)].

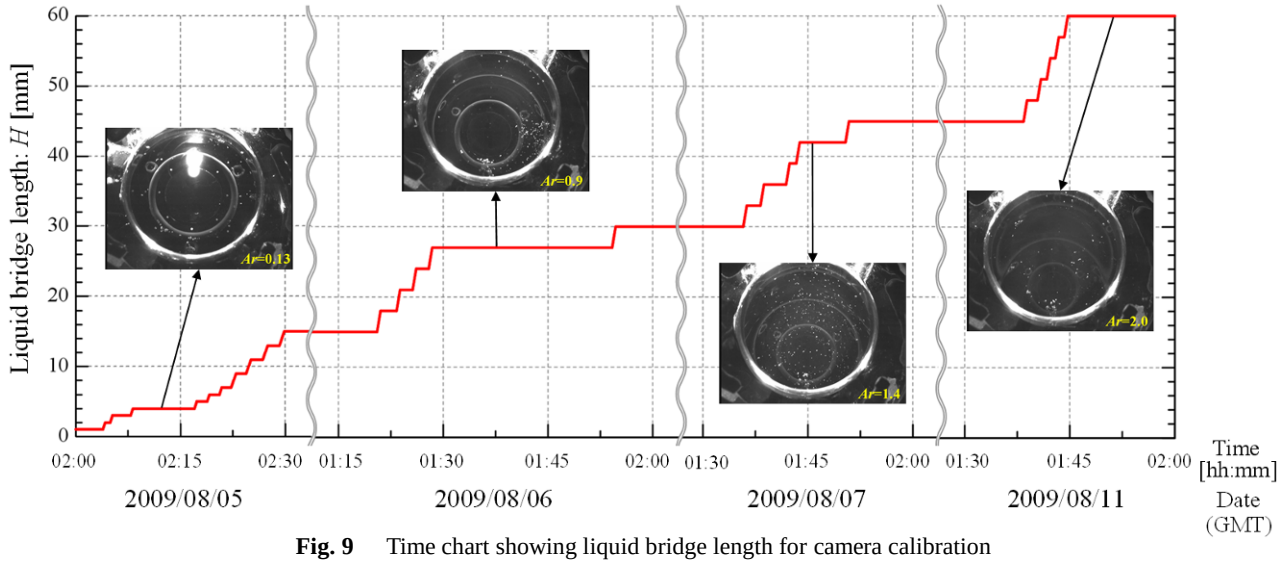

Fig. 9 Time chart showing liquid bridge length for camera calibration

The solution for the camera parameters requires a set of calibration data. They are provided as white calibration dots marked on the surface of the cooled disk. Their 3-D position in the absolute coordinate system and their corresponding 2-D positions in the image coordinate system are given. **Figure 8** shows the layout of the calibration dots used in MEIS-2. A total of 23 calibration dots are marked on the traversable cooled disk. **Figure 9** shows the relation between the liquid bridge length and the timing when each calibration image is obtained. A total of 26 images at different disk positions are acquired. For image acquisition, the cooled disk is traversed in a step-wise manner as shown in the figure.

The residual errors in the solution for the camera parameters are shown in **Table 1**. The values are projection errors. The errors in X and Y directions for all CCD cameras are less than 1 pixel, indicating that the present camera calibration is done quite accurately.

Table 1 Projection errors in camera parameters

	X-direction	Y-direction	Combined
Camera#1	0.47pixel	0.54pixel	0.80pixel
Camera#2	0.56pixel	0.62pixel	0.94pixel
Camera#3	0.56pixel	0.58pixel	0.90pixel

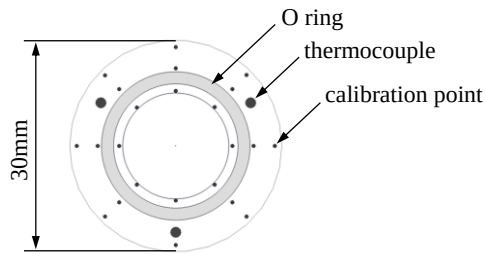

Fig. 8 Calibration dots on the cooled disk

4. Result

4.1 Uncertainty analysis

Measurement uncertainties in the present 3-D PTV are systematically evaluated according to the method described in ANSI/ASME PTC19.1[8]. The uncertainty interval at 95 percent coverage is calculated as $U_{RSS}=(B^2+(tS)^2)^{0.5}$, where B is the bias limit, S is the precision index and t is the student t value. In particular, (1) the fidelity of particle motion to fluid motion and (2) the uncertainty of 3-D position measurement are considered.

The fidelity of particle motion to fluid motion is evaluated by considering the frequency response and the effect of centrifugal force. The particle motion in the fluid can be described by the Basset-Boussinesq-Oseen equation. According to Hjelmfelt and Mockros[9] who solved this equation for particle motions in periodic fluid motions, the fidelity under the condition of MIES is shown to be sufficiently good. The effect of centrifugal force on particle motion is also very small. However, the particles tend to be accumulated gradually in the region near the free surface of the liquid bridge and therefore a void region where the number of particles is small grows in the core of the liquid bridge, particularly for low Ar.

Uncertainty of the 3-D position measurement was evaluated by measuring the 3-D position of each calibration dot and by comparing it with its given 3-D position. **Table 2** shows the total uncertainties for different ranges of z-position.

Table 2 Uncertainties of 3-D position

z[mm]	$U_{RSS\text{-}x}$ [mm]	$U_{RSS\text{-}y}$ [mm]	$U_{RSS\text{-}z}$ [mm]	ρ_N[/cm^3]
60-45	±0.10	±0.08	±0.39	19.2
45-30	±0.12	±0.10	±0.65	11.0
30-15	±0.12	±0.12	±1.01	11.0
15-0	±0.14	±0.19	±1.31	9.4

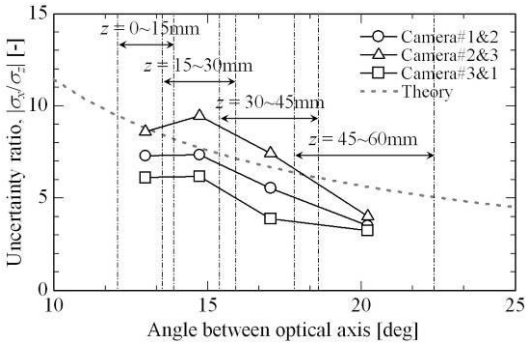

Fig. 10 Uncertainty ratio between z and x direction as a function of the viewing angle between two cameras

In this table, ρ_N is the number density of calibration dots in the measuring volume. As the distance between CCD cameras and the measuring position increases, the measurement uncertainty increases. This deterioration is caused by the limited depth of field and by the decrease of effective viewing angle between CCD cameras. Moreover the calibration dots at z=0-15mm are not focused well and therefore the pixel errors in image coordinate become larger. In general, the uncertainty in z-direction increases with decreasing viewing angle between cameras. It is indicated in **Fig. 10**, in which the uncertainty ratio between axial and radial directions in the camera coordinate is shown as a function of the angle between optical axes of the cameras. As expected, the uncertainty ratio decreases with the angle and it becomes about four at an angle of 20deg. For the angle smaller than 14deg, the uncertainty ratio decreases with decreasing angle. This is because of the rapid increase of $U_{RSS\text{-}x}$, the uncertainty in x direction, due to the defocusing mentioned above.

4.2 Result of 3-D PTV

4.2.1 *Ar*=1.25

Figure 11 is the result of the 3-D PTV measurement of the thermocapillary convection. The conditions are Ar=1.25 and ΔT=2.9°C, ($\Delta T/\Delta T_c$=0.54, Ma=1.90×10^4). The flow is steady for this ΔT and the presence of an axisymmetric 2-D velocity field is evident as seen from the top view. **Figure 12** shows the comparison between the present result and a CFD result. The pattern of the stream lines looks very similar and two vortices exist. Such a flow pattern is called the multi-roll structure and it is considered to be unique to high Ar liquid bridges. Figure 12 also shows the axial velocity profiles at several radial positions. Reasonable agreement is recognized.

4.2.2 *Ar*=1.5

Figure 13 is the visualization of particle trajectories which are generated by the superposition of particle images in the duration of 15s. The conditions are Ar=1.5 and $\Delta T >> \Delta T_c$, (ΔT=11.2°C, $\Delta T/\Delta T_c$=3.7, Ma=9.45×10^4). **Figure 14** is the result of 3-D PTV at the same instance for the visualization shown in **Fig. 13**. The flow structures seen from two orthogonal directions are indicated and oscillatory complex flow patterns are observed. The oscillation of the convection is seen to occur in a fixed direction. Such a flow pattern is called a standing wave with mode number m=1.

5. Summary

The flow fields associated with oscillatory thermocapillary convection in large liquid bridges have been studied by using the 3-D PTV technique. The microgravity environment in the International Space Station (ISS) was used to generate large liquid bridges in the Fluid Physics Experiment Facility (FPEF). A modified multi-frame particle tracking for 3-D reconstruction of particle trajectories was developed. As a result, accurate and reliable particle trajectories and associated velocity field in the thermocapillary convection were obtained. The uncertainty of the measurement accuracy was evaluated according to the method described in ANSI/ASME PTC19.1. The flow field in a laminar state for Ar=1.25 and oscillatory state for Ar=1.5 were measured.

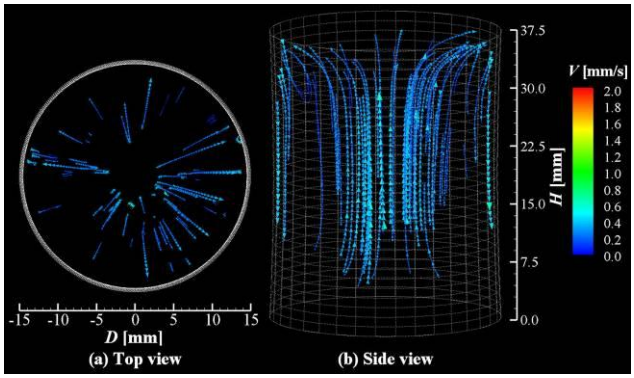

Fig. 11 3-D particle trajectories in steady state

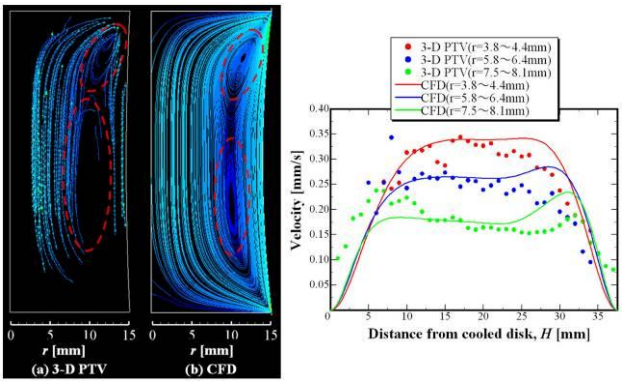

Fig. 12 Comparison with CFD result

Fig. 13 Particle trajectories for 15 second

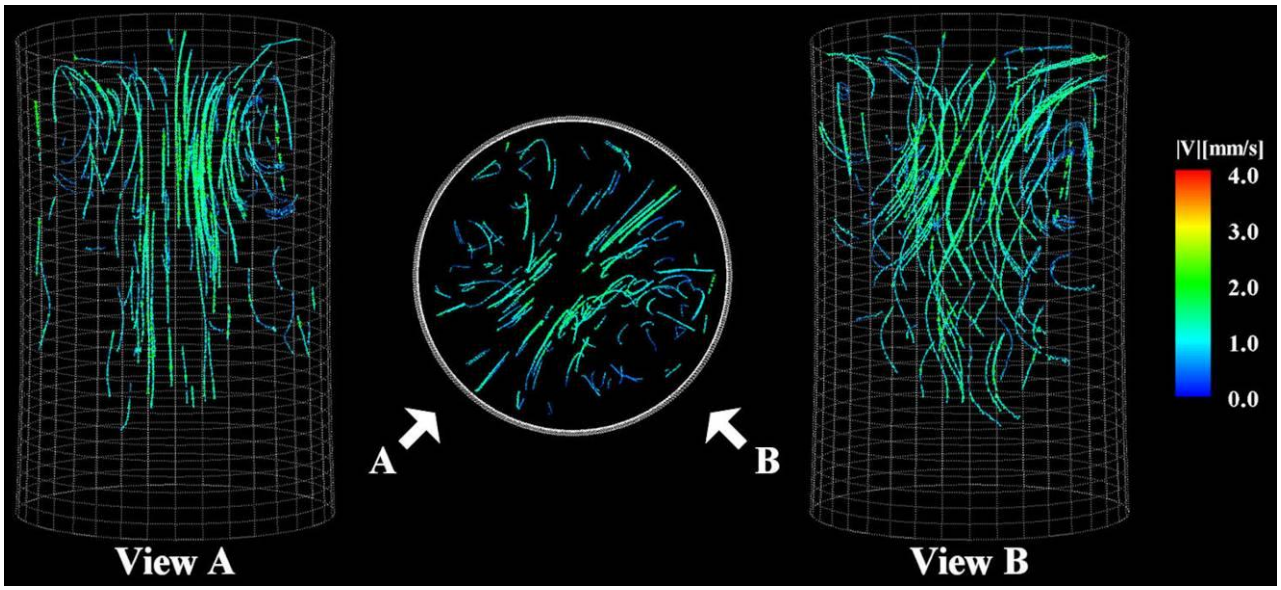

Fig. 14 Result of 3-D PTV for oscillatory state

Acknowledgement

The author would like to thank JAXA and the members of MEIS for their assistance to perform this study. The authors also acknowledge that a part of this study was supported by Grant-in Aid for Scientific Research (B#21360101) from the Japan Society for Promotion of Science (JSPS).

References

1) H. Kawamura, K. Nishino, S. Matsumoto and I. Ueno: Proc. 14th Int. Heat Transfer Conf., Washington, Aug 8-13, 2010.
2) M. Nishimura, I. Ueno, K. Nishino and H. Kawamura: Exp. Fluids, **38** (2005) 285.
3) H. Kawamura, K. Saita, K. Nishino, M. Yamamoto, S. Yoda, T. Nakamura, T. S. Morita, K. Kawasaki and H. Tamaoki: J. Jpn. Soc. Microgravity Appl., **14** (1997) 34.
4) K. Nishino, H. Kawamura, T. Emori, Y. Iijima, K. Kawasaki, K. Makino, S. Yoda and H. Kawasaki: J. Jpn. Soc. Microgravity Appl., **15** (1998) 158.
5) T. Yano, K. Nishino, H. Kawamura, M. Ohnishi, I. Ueno, S. Matsumoto, S. Yoda and T. Tanaka: Proc. 14th Int. Symp. Flow Visualization, Daegu, Korea, June 20-24, 2010.
6) K. Nishino, N. Kasagi and M. Hirata: Transaction of the ASME .J. Fluid Eng., **111** (1989) 384.
7) K. Nishino, T. Yamawaki and M. Takami: J. Jpn. Soc. Microgravity Appl., **12** (1995) 205.
8) ANSI/ASME PTC 19.1-1985, 1986.
9) A. T. Hjelmfelt and L. F. Mockros: Appl. Sci. Res., **16** (1966) 61.

(Received 22 Oct. 2010; Accepted 12 Sept. 2011)